Transmissive and Transflective Blue-Phase LCDs With Double-Layer IPS Electrodes

Yan Li, Shuaijia Huang, Na Rong, Jian-Gang Lu, Chao Ping Chen, Xiao Li, Pengcheng Zhou, Yachao Yuan, Shuxin Liu, Gufeng He, and Yikai Su, *Senior Member, IEEE*

***Abstract*—A double-layer in-plane-switching electrode design is proposed for transmissive and transflective blue-phase liquid crystal displays. The new design significantly reduces the operating voltage in transmissive display by 60%; in transflective displays where the bottom-layer electrodes are made of conductive reflectors, it increases transmittance to 98%, achieves single gamma driving and enhances sunlight readability.**

***Index Terms*—Blue phase, liquid crystal displays, transflective.**

I. Introduction

BLUE-PHASE liquid crystal (BPLC) [1]–[7] has become an attractive candidate for next-generation display technology due to several features: 1) submillisecond gray-to gray response [8], 2) no need for alignment, 3) cell gap insensitivity in in-plane-switching (IPS) mode, and 4) wide viewing angle. The fast response time effectively eliminates motion image blur; moreover, it enables color sequential display using red, green and blue light-emitting diodes, and thus both the optical efficiency and resolution density can be increased by 3 times [9]. The conventional IPS blue-phase liquid crystal display (BPLCD) [4], which utilizes horizontal fringe electric fields, inherently has a wide viewing angle. Since the fringe fields have limited penetration depth into the LC layer, the IPS structure is insensitive to cell gap variation. However, it requires a high operating voltage ($\sim 50\ V_{rms}$). In addition, hysteresis [10], residual birefringence, long term stability, etc. need to be addressed before the application of BPLCDs can be practically implemented.

Recently, great efforts have been made to lower the operating voltage of BPLCDs [11]–[23], such as protrusion electrodes [6], [11]–[13], wall-shaped electrodes [15]–[18], corrugated electrodes [19] and enhanced protrusion electrodes [20]. The operating voltage has been reduced from $\sim 50\ V_{rms}$ to less than $10\ V_{rms}$. However, the nonplanar electrode fabrication is complicated and difficult to realize. A vertical-field-switching (VFS) BPLCD [21] was proposed using simple planar electrodes, however, complicated optical films are needed to achieve a wide viewing angle [24], [25]. A BPLCD with an etched substrate [26]–[28] generates double-penetrating fringe fields, resulting in a lowered operating voltage. But due to the limited penetration depth of the single-layer IPS electrodes, the voltage reduction is less effective.

In this paper, we propose a double-layer IPS electrode structure for BPLCDs. Each layer of the planar ITO electrodes generates double-penetrating fields, therefore, the total field penetrating depth is significantly enlarged and the operating voltage is lowered. The electro-optical (EO) properties of the proposed design under different electrode configurations and substrate etching depths are evaluated and analyzed. Moreover, the design is also useful for transflective (TR) BPLCDs [20], [29]–[35] if the bottom electrodes are made of conductive reflectors. The TR BPLCD can achieve high transmittance, single gamma driving and a wide viewing angle.

II. Device Structure

Fig. 1(a) depicts the device structure with single-layer IPS electrodes and an etched substrate [26], where w is the electrode width, l the spacing between adjacent electrodes, and h the etching depth of the substrate. The LC cell is sandwiched between two crossed polarizers. The strip electrodes are orientated 45° in respect to the transmission axes of the polarizers. When a voltage is applied between adjacent electrodes, fringe fields are generated, penetrating into both sides of the substrate. So the BPLC in the etched part of the substrate also contributes to phase retardation and transmittance. Thus the driving voltage is lowered compared to a conventional IPS BPLCD without etching. However, the penetration depth is limited by electrode dimensions. For a single-layer etched IPS BPLCD with $w = 2\ \mu$m and $l = 4\ \mu$m, the downward penetration depth is around 1 μm. With a larger electrode dimension, $w = 5\ \mu$m and $l = 10\ \mu$m, the downward penetration depth is $\sim 2\ \mu$m [26].

Fig. 1(b) depicts the proposed structure where there are two layers of planar electrodes. Here w_1 is the width of top-layer electrodes, w_2 the width of bottom-layer electrodes; h_1 is the vertical distance between the top and bottom-layer electrodes, h_2 is the vertical distance between the bottom-layer electrodes and the substrate surface as shown in Fig. 1(b); and l is the spacing between adjacent top-layer electrodes. In this design, both top and bottom-layer electrodes generate fringe fields

Manuscript received June 17, 2015; revised August 05, 2015; accepted August 12, 2015. Date of publication August 28, 2015; date of current version February 02, 2016. This work was supported by 973 Program under Grant 2013CB328803, National Natural Science Foundation of China under 61405114, and Science and Technology Commission of Shanghai Municipality under Grant 14ZR1422300.

The authors are with the National Engineering Laboratory of TFT-LCD Materials and Technologies, Department of Electronic Engineering, Shanghai Jiao Tong University, Shanghai 200240, China (e-mail: yan.li@sjtu.edu.cn).

Color versions of one or more of the figures are available online at http://ieeexplore.ieee.org.

Digital Object Identifier 10.1109/JDT.2015.2470086

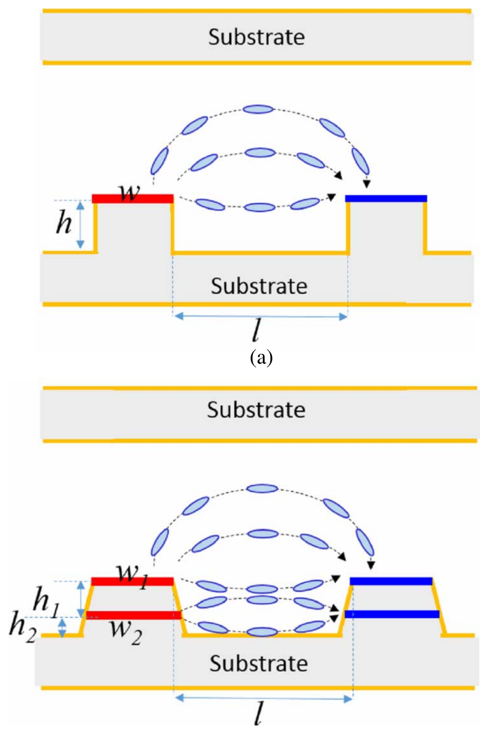

Fig. 1. Device structures of (a) a single-layer etched IPS cell and (b) a double-layer IPS cell.

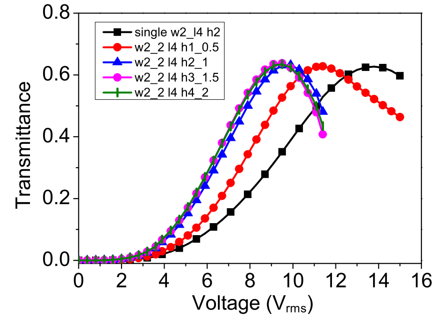

Fig. 2. Simulated VT curves of the BPLC cells with $w = w_1 = w_2 = 2\ \mu$m and $l = 4\ \mu$m.

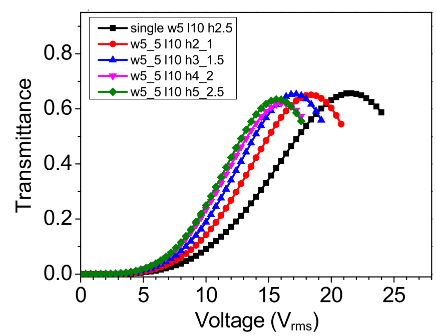

Fig. 3. Simulated VT curves of the BPLC cells with $w = w_1 = w_2 = 5\ \mu$m and $l = 10\ \mu$m.

with double penetration, so that the total phase retardation is increased and the operating voltage significantly reduced.

III. Results

To evaluate the performances of the proposed structure, we carried out electro-optical simulations using commercial software Dimos (AUTRONIC-MELCHERS GmbH, Germany). The Kerr constant is assumed as 33.1 nm/V^2 ($\lambda = 550$ nm), the dielectric constants of the BPLC are $\varepsilon_{r//} = 311$ and $\varepsilon_{r\perp} = 15$, respectively, as reported in [36]. The saturation birefringence of the BPLC mixture used for simulation is 0.14.

Fig. 2 shows the voltage-dependent transmittance (VT) curves with different electrode configurations. The black curve is for a single-layer etched IPS structure with $w = 2\ \mu$m and $l = 4\ \mu$m. From [26], we learn that as long as the etching depth is larger than the apparent penetration depth (1 μm with $w = 2\ \mu$m, $l = 4\ \mu$m), the VT curve is insensitive to h. Hence, here a large etching depth $h = 2\ \mu$m is chosen. The operating voltage V_p is around 13.6 V_{rms}, which is lower than that in a conventional IPS cell with the same electrode dimension (23 V_{rms}, not shown in the figure).

The other VT curves are for the double-layer-electrode structure. The legend "w2_2 l4 h1_0.5" designates a configuration with $w_1 = w_2 = 2\ \mu$m, $l = 4\ \mu$m, $h_1 = 1\ \mu$m and $h_2 = 0.5\ \mu$m. In such a structure, h_1 confines both the top and bottom-layer fringe fields, while h_2 only confines the bottom fields. For different configurations, h_1 and h_2 vary but are kept at a 2:1 ratio. As h_1 and h_2 increase, the operating voltage decreases accordingly. When $h_1 = 2\ \mu$m, and $h_2 = 1\ \mu$m, V_p drops to below 10 V_{rms}, with no noticeable change in transmittance. When $h_1 = 3\ \mu$m, $h_2 = 1.5\ \mu$m, V_p is further decreased and saturates at 9 V_{rms}.

Fig. 3 shows the VT curves of several configurations with $w = w_1 = w_2 = 5\ \mu$m and $l = 10\ \mu$m. For the single-layer structure, h is 2.5 μm, which is larger than the corresponding penetrating depth ($\sim 2\ \mu$m). A similar trend in operating voltage and transmittance is observed as the etching depths of the double-layer structure increase. A larger dimension of $w + l$ results in a larger penetration depth. When $h_1 = 5\ \mu$m, $h_2 = 2.5\ \mu$m, V_p drops to a saturation value ($\sim 15\ V_{rms}$).

In Fig. 4, the electric field intensity distributions in the BPLC layer are plotted at the operation voltage 9.8 V_{rms} for a BPLC cell with $w_1 = w_2 = 2\ \mu$m, $l = 4\ \mu$m, $h_1 = 2\ \mu$m and $h_2 = 1\ \mu$m. The low operating voltage could reduce the peak electric field which occurs near the edges of the electrodes, and thus help suppress electrostriction effect and hysteresis [37].

In Fig. 5, the impact of the dielectric constant of the substrate material on the operating voltage is studied. The BPLC cell parameters are kept as $w = w_1 = w_2 = 2\ \mu$m, $l = 4\ \mu$m, $h_1 = 2\ \mu$m, and $h_2 = 1\ \mu$m, and the dielectric constant of the substrate ε_r varies. As ε_r is enlarged 10 times from 3.8 to 38, a small voltage reduction is achieved from 9.8 V_{rms} to 9.6 V_{rms}. In [38], higher-dielectric insulating materials with $\varepsilon_r = 80$ and 120 have been adopted. As shown in Fig. 5, when ε_r further increases, the operating voltage further decreases as well, but the voltage reduction is not large even at a high $\varepsilon_r = 120$.

We also study the EO performances of the proposed design with different w_1/w_2 ratios. First, we keep the top electrode width w_1 and top spacing l fixed, but vary the bottom electrode width w_2. As shown in Fig. 6(a), for those with the same

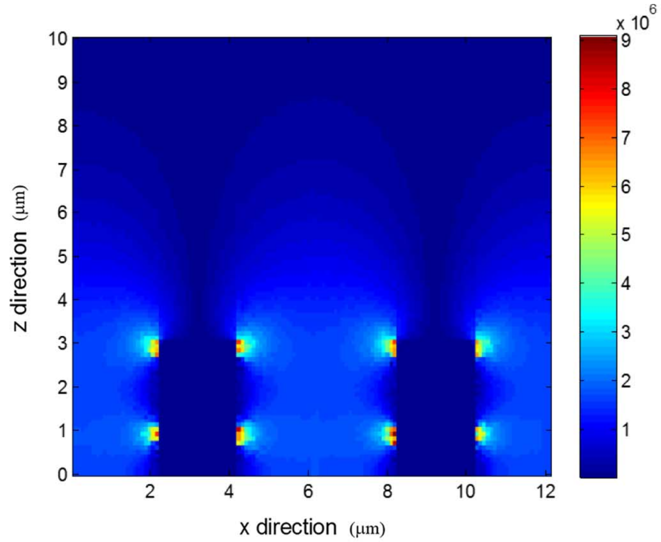

(a)

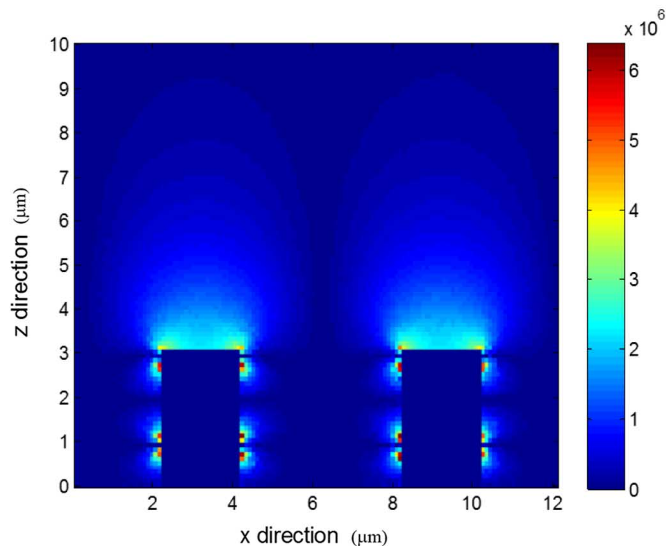

(b)

Fig. 4. Simulated horizontal ($|E_x|$) and vertical ($|E_z|$) electric field distributions in the BPLC layer (electric field in the substrates not shown). The cell parameters are $w = w_1 = w_2 = 2\ \mu$m, $l = 4\ \mu$m, $h_1 = 2\ \mu$m, and $h_2 = 1\ \mu$m. (a) $|E_x|$. (b) $|E_z|$.

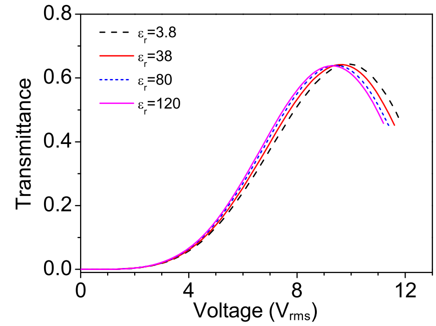

Fig. 5. Simulated VT curves of BPLC cells with $w = w_1 = w_2 = 2\ \mu$m, $l = 4\ \mu$m, $h_1 = 2\ \mu$m, and $h_2 = 1\ \mu$m as the dielectric constant of the substrate varies.

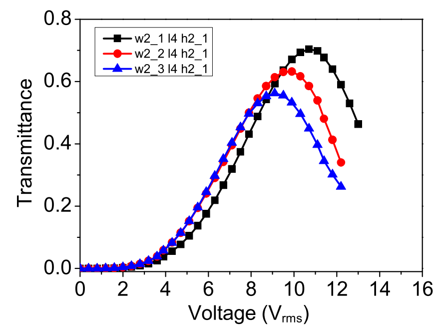

(a)

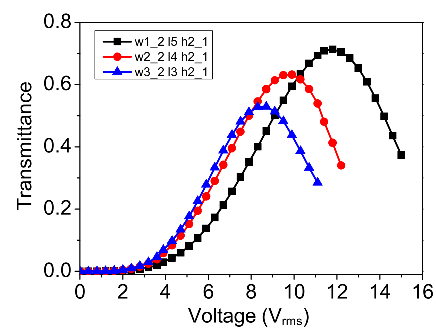

(b)

Fig. 6. Simulated VT curves of BPLC cells (a) with $w_1 = 2\ \mu$m and different w_2 and (b) with $w_2 = 2\ \mu$m and different w_1.

$w_1 = 2\ \mu$m, the one with the smallest $w_2 (w_2 = 1\ \mu$m) has the highest operating voltage (10.7 V_{rms}) and highest transmittance; and the one with the largest $w_2 (w_2 = 3\ \mu$m) has the lowest voltage (9.1 V_{rms}) and lowest transmittance. For such a structure, a larger w_2 indicates smaller bottom spacing, hence stronger fringe fields are generated in the LC region between the bottom-layer electrodes. As a result, a lower voltage is required to achieve sufficient total phase retardation. On the other hand, as w_2 gets larger, more substrate material takes space, leaving a smaller effective LC region between the bottom-layer electrodes. Thus, the average transmittance contributed by both top and bottom LC layers becomes lower.

Fig. 6(b) shows the VT curves of the structure with the same w_2, $w_1 + l$, but different w_1. A similar trend in the variation of operating voltage and transmittance is observed. However, compared to the previous case, the variation of the top-layer electrode width w_1 seems to have a more significant impact on the operating voltage. The peak voltage is reduced to 8.7 V_{rms} with $w_1 = 3\ \mu$m, and increased to 11.8 V_{rms} with $w_1 = 1\ \mu$m. The more pronounced change in the voltage may arise from the fact that, the top-layer electrodes play a predominant role in the EO switching. The reason is explained as follows. For a single layer etched electrode structure, since the dielectric constant of the BPLC is much larger than that of the substrate [36], the electric potential changes more rapidly in the substrate than in the BPLC layer. Therefore, the electric fields penetrate deeper upwards into the BPLC layer ($\sim 2\ \mu$m) [39], and penetrate sallower downwards ($\sim 1\ \mu$m) [26]. As in the double-layer structure, the top-layer electrodes have a larger total penetration depth ($3\ \mu$m $= 2\ \mu$m $+ 1\ \mu$m) than the bottom-layer electrodes ($2\ \mu$m $= 1\ \mu$m $+ 1\ \mu$m), therefore, the top-layer electrode dimension has a more pronounced influence on the operating voltage than the bottom layer.

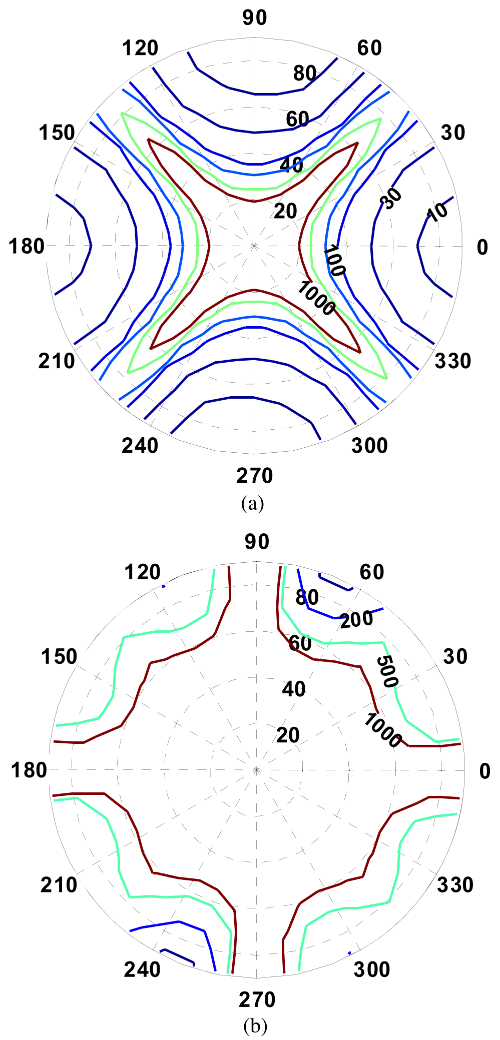

Fig. 7. Isocontrast plots of a proposed BPLC cell structure (a) without and (b) with a biaxial compensation film, respectively. The cell parameters are $w = w_1 = w_2 = 2\ \mu$m, $l = 4\ \mu$m, $h_1 = 2\ \mu$m, and $h_2 = 1\ \mu$m.

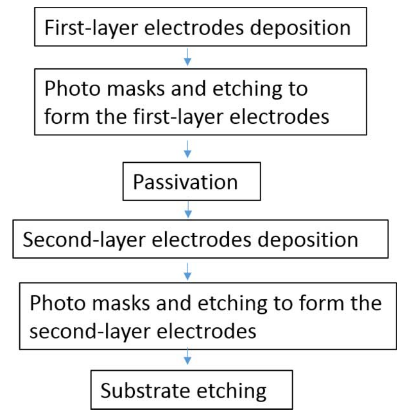

Fig. 8. Flowchart of one possible fabrication approach.

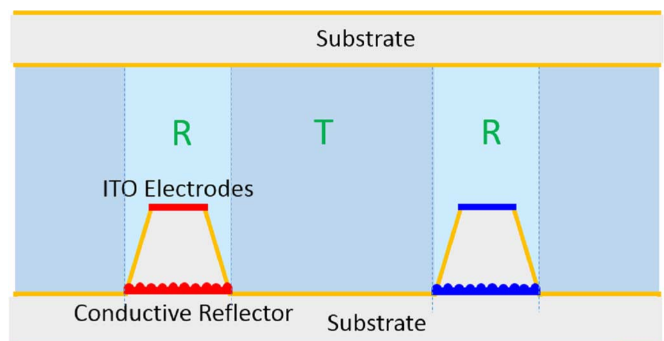

Fig. 9. Device structure of a transflective BPLCD using double-layer IPS electrodes.

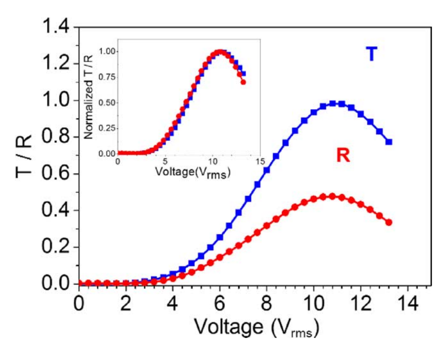

Fig. 10. Voltage-dependent transmittance and reflectance curves of a transflective BPLCD.

By compensating the polarization rotation effect of BPLC, the display could achieve an excellent dark state and a high contrast ratio of over ~4000:1 can be achieved easily [40]. Here we used broadband wide-view circular polarizers [41] to eliminate the effect of polarization rotation. Fig. 7(a) and (b) plots the isocontrast plots of a BPLC cell without and with a biaxial compensation film, respectively. The cell parameters are $w = w_1 = w_2 = 2\ \mu$m, $l = 4\ \mu$m, $h_1 = 2\ \mu$m, and $h_2 = 1\ \mu$m.

The fabrication of the double-layer structure could be realized by adopting multiple photo mask process architecture and slit photolithography. The electrode patterns could be obtained in a fashion similar to [42]–[44]. The substrate can further be etched to create depths as in [28]. Fig. 8 shows the flowchart of a possible fabrication approach.

The proposed structure can also be used in transflective BPLCDs which greatly enhance sunlight readability outdoors. As shown in Fig. 9, the top layer IPS electrodes are made of transparent ITO electrodes, while the bottom-layer IPS electrodes are made of conductive reflectors. Therefore, the LC above the reflective electrodes works in the reflective (R) mode, while the other operates in the transmissive (T) mode as shown in the figure. In the T region, there are fringe fields with large horizontal component generated by both layers of electrodes, thus the optical phase retardation is larger than that in the R region at the same voltage. On the other hand, in the R region, the fringe fields are mainly generated by the top-layer electrodes, so the accumulated phase retardation is relatively small. Since ambient light passes through R region twice, while the backlight travels through T region only once, the optical phase retardations are matched between the two regions.

Fig. 10 shows the voltage-dependent transmittance and reflectance curves with $w_1 = 2\ \mu$m, $w_2 = 4\ \mu$m, $l = 5\ \mu$m, $h_1 = 1.8\ \mu$m and $h_2 = 0$. By converting the most effective region into T region, the transmittance is increased to 98%. At 10.8 V_{rms}, both transmittance and reflectance reach the peak, and from the inserted figure, one can see that the normalized transmittance and reflectance match very well with each other, indicating single gamma driving is enabled. By using biaxial compensation films and wide-angle circular polarizers, a wide viewing angle could be achieved for both T and R regions [20], [29].

IV. Conclusion

We have proposed a double-layer IPS electrode structure for BPLCDs. In transmissive BPLCDs, the proposed structure could reduce the operating voltage by 30% compared with a single-layer etched IPS structure, and by 60% compared with a conventional IPS structure, whereas a similar transmittance is maintained. In transflective BPLCDs, the proposed structure could achieve high transittance (∼98%), low voltage, well matched transmittance and reflectance, and good sunlight readability.

References

[1] H. Kikuchi, M. Yokota, Y. Hisakado, H. Yang, and T. Kajiyama, "Polymer-stabilized liquid crystal blue phases," *Nat. Mater.*, vol. 1, no. 1, pp. 64–68, 2002.

[2] S. W. Choi, S. I. Yamamoto, Y. Haseba, H. Higuchi, and H. Kikuchi, "Optically isotropic-nanostructured liquid crystal composite with high Kerr constant," *Appl. Phys. Lett.*, vol. 92, no. 4, 2008, Art ID 043119.

[3] Y. Haseba, S. I. Yamamoto, K. Sago, A. Takata, and H. Tobata, "Invited paper: Low voltage polymer stabilized blue phase liquid crystals," in *SID Int. Symp. Dig. Tech. Papers*, 2013, vol. 44, pp. 254–257.

[4] Z. Ge, S. Gauza, M. Jiao, H. Xianyu, and S. T. Wu, "Electro-optics of polymer-stabilized blue phase liquid crystal displays," *Appl. Phys. Lett.*, vol. 94, no. 10, 2009, Art ID 101104.

[5] M. Wittek, N. Tanaka, D. Wilkes, M. Bremer, D. Pauluth, J. Canisius, A. Yeh, R. Yan, K. Skjonnemand, and M. Klasen-Memmer, "New materials for polymer stabilized blue phase," in *SID Int. Symp. Dig. Tech. Papers*, 2012, vol. 43, pp. 25–28.

[6] H. Lee, H. J. Park, O. J. Kwon, S. J. Yun, J. H. Park, S. Hong, and S. T. Shin, "Invited paper: The world's first blue phase liquid crystal display," in *SID Int. Symp. Dig. Tech. Papers*, 2011, vol. 42, pp. 121–124.

[7] Y. Chen and S. T. Wu, "Recent advances on polymer-stabilized blue phase liquid crystal materials and devices," *J. Appl. Polym. Sci.*, vol. 131, no. 13, 2014.

[8] K. M. Chen, S. Gauza, H. Xianyu, and S. T. Wu, "Submillisecond gray-level response time of a polymer-stabilized blue-phase liquid crystal," *J. Display Technol.*, vol. 6, no. 2, pp. 49–51, 2010.

[9] Y. Hirakata, D. Kubota, A. Yamashita, T. Ishitani, T. Nishi, H. Miyake, H. Miyairi, J. Koyama, S. Yamazaki, and T. Cho, "A novel field sequential blue phase mode AMLCD," *J. Soc. Inf. Display*, vol. 20, no. 1, pp. 38–46, 2012.

[10] K. M. Chen, S. Gauza, H. Xianyu, and S. T. Wu, "Hysteresis effects in blue-phase liquid crystals," *J. Display Technol.*, vol. 6, no. 8, pp. 318–322, 2010.

[11] S. Yoon, M. Kim, M. Su Kim, B. Gyun Kang, M. K. Kim, A. Kumar Srivastava, S. Hee Lee, Z. Ge, L. Rao, and S. Gauza, "Optimisation of electrode structure to improve the electro-optic characteristics of liquid crystal display based on the Kerr effect," *Liq. Cryst.*, vol. 37, no. 2, pp. 201–208, 2010.

[12] L. Rao, Z. Ge, S. T. Wu, and S. H. Lee, "Low voltage blue-phase liquid crystal displays," *Appl. Phys. Lett.*, vol. 95, no. 23, 2009, Art ID 231101.

[13] Z. Su, Y. Chen, J. Lu, and X. Tang, "High-transmittance polymer-stabilised blue-phase liquid crystal display with double-sided protrusion electrodes," *Liq. Cryst.*, vol. 40, no. 7, pp. 976–979, 2013.

[14] Y. Sun, Y. Zhao, Y. Li, P. Li, and H. Ma, "Optimisation of in-plane-switching blue-phase liquid crystal display," *Liq. Cryst.*, vol. 41, no. 5, pp. 717–720, 2014.

[15] M. Kim, M. S. Kim, B. G. Kang, M. K. Kim, S. Yoon, S. H. Lee, Z. Ge, L. Rao, S. Gauza, and S. T. Wu, "Wall-shaped electrodes for reducing the operation voltage of polymer-stabilized blue phase liquid crystal displays," *J. Phys. D: Appl. Phys.*, vol. 42, no. 23, 2009, Art ID 235502.

[16] M. S. Kim, M. Kim, J. H. Jung, K. S. Ha, S. Yoon, E. G. Song, A. K. Srivastava, S. W. Choi, G. D. Lee, and S. H. Lee, "Blue phases liquid crystal cell driven by strong in-plane electric field," in *SID Int. Symp. Dig. Tech. Papers*, 2009, vol. 40, pp. 1615–1618.

[17] F. Zhou, Q. Wang, D. Wu, and J. Cui, "Polymer-stabilized blue phase liquid crystal display with slanted wall-shaped electrodes," *Chin. Opt. Lett.*, vol. 10, no. 2, 2012, Art ID 022301.

[18] C. Y. Tsai, F. C. Yu, Y. F. Lan, P. J. Huang, S. Y. Lin, Y. T. Chen, T. I. Tsao, C. T. Hsieh, B. S. Tseng, C. W. Kuo, C. H. Lin, C. C. Kuo, C. H. Chen, H. Y. Hsieh, C. T. Chuang, N. Sugiura, C. L. Lin, and M. H. Cheng, "Distinguished paper: A novel blue phase liquid crystal display applying wall-electrode and high driving voltage circuit," in *SID Int. Symp. Dig. Tech. Papers*, 2015, vol. 46, no. 1, pp. 542–544.

[19] M. Jiao, Y. Li, and S. T. Wu, "Low voltage and high transmittance blue-phase liquid crystal displays with corrugated electrodes," *Appl. Phys. Lett.*, vol. 96, no. 1, 2010, Art ID 011102.

[20] Y. Li and S. T. Wu, "Transmissive and transflective blue-phase LCDs with enhanced protrusion electrodes," *J. Display Technol.*, vol. 7, no. 7, pp. 359–361, 2011.

[21] H. C. Cheng, J. Yan, T. Ishinabe, and S. T. Wu, "Vertical field switching for blue-phase liquid crystal devices," *Appl. Phys. Lett.*, vol. 98, no. 26, 2011, Art ID 261102.

[22] P. Li, Y. Sun, Y. Zhao, and Q. Wang, "High transmittance blue-phase liquid crystal displays with slit-shaped electrode," *Liq. Cryst.*, vol. 40, no. 10, pp. 1417–1421, 2013.

[23] Y. Chen, Y. Sun, and G. Yang, "Low voltage and high transmittance blue-phase LCDs with double-side in-plane switching electrodes," *Liq. Cryst.*, vol. 38, no. 5, pp. 555–559, 2011.

[24] H. C. Cheng, J. Yan, T. Ishinabe, C. H. Lin, K. H. Liu, and S. T. Wu, "Wide-view vertical field switching blue-phase LCD," *J. Display Technol.*, vol. 8, no. 11, pp. 627–633, 2012.

[25] J. Yan, D. Xu, H. C. Cheng, S. T. Wu, Y. F. Lan, and C. Y. Tsai, "Turning film for widening the viewing angle of a blue phase liquid crystal display," *Appl. Opt.*, vol. 52, no. 36, pp. 8840–8844, 2013.

[26] L. Rao, H. C. Cheng, and S. T. Wu, "Low voltage blue-phase LCDs with double-penetrating fringe fields," *J. Display Technol.*, vol. 6, no. 8, pp. 287–289, 2010.

[27] D. Xu, Y. Chen, Y. Liu, and S. T. Wu, "Refraction effect in an in-plane-switching blue phase liquid crystal cell," *Opt. Express*, vol. 21, no. 21, pp. 24721–24735, 2013.

[28] C. Y. Tsai, T. J. Tseng, L. Y. Wang, F. C. Yu, Y. F. Lan, P. J. Huang, S. Y. Lin, K. M. Chen, B. S. Tseng, C. W. Kuo, C. H. Lin, J. K. Lu, and N. Sugiura, "Invited paper: Polymer-stabilized blue phase liquid crystal displays applying novel groove cell structure," in *SID Int. Symp. Dig. Tech. Papers*, 2013, vol. 44, no. 1, pp. 182–183.

[29] Y. Li, M. Jiao, and S. T. Wu, "Transflective display using a polymer-stabilized blue-phase liquid crystal," *Opt. Express*, vol. 18, no. 16, pp. 16486–16491, 2010.

[30] E. W. Zhong, S. B. Ni, J. Tan, Y. Song, S. Y. Liu, Y. J. Wang, J. L. Zhu, and J. G. Lu, "A transflective display using blue phase liquid crystal," *J. Display Technol.*, vol. 10, no. 5, pp. 357–361, 2014.

[31] F. Zhou, J. P. Cui, Q. H. Wang, D. H. Li, and D. Wu, "A single-cell-gap transflective display using a blue-phase liquid crystal," *J. Display Technol.*, vol. 7, no. 4, pp. 170–173, 2011.

[32] H. Q. Cui, Z. C. Ye, W. Hu, X. Lin, T. Chung, T. S. Jen, and Y. Q. Lu, "Single cell gap polymer-stabilized blue-phase transflective LCDs using internal nanowire grid polarizer," *J. Inf. Disp.*, vol. 12, no. 3, pp. 115–119, 2011.

[33] J. P. Cui, F. Zhou, Q. H. Wang, D. Wu, and D. H. Li, "Transflective blue-phase liquid crystal display using an etched in-plane switching structure," *J. Display Technol.*, vol. 7, no. 7, pp. 398–401, 2011.

[34] D. Wu, Q. H. Wang, F. Zhou, J. P. Cui, and C. Q. Song, "Low voltage and high optical efficiency single-cell-gap transflective display using a blue-phase liquid crystal," *J. Display Technol.*, vol. 7, no. 8, pp. 459–462, 2011.

[35] P. Li, Y. Sun, and Q. Wang, "A transflective and viewing angle controllable blue-phase liquid crystal display," *Liq. Cryst.*, vol. 40, no. 8, pp. 1024–1027, 2013.

[36] Y. Chen, D. Xu, S. T. Wu, S. I. Yamamoto, and Y. Haseba, "A low voltage and submillisecond-response polymer-stabilized blue phase liquid crystal," *Appl. Phys. Lett.*, vol. 102, no. 14, 2013, Art ID 141116.

[37] L. Rao, J. Yan, S. T. Wu, Y. C. Lai, Y. H. Chiu, H. Y. Chen, C. C. Liang, C. M. Wu, P. J. Hsieh, and S. H. Liu, "Critical field for a hysteresis-free BPLC device," *J. Display Technol.*, vol. 7, no. 12, pp. 627–629, 2011.

[38] C. T. Lee, Y. Li, H. Y. Lin, and S. T. Wu, "Design of polarization-insensitive multi-electrode GRIN lens with a blue-phase liquid crystal," *Opt. Express*, vol. 19, no. 18, pp. 17402–17407, 2011.

[39] Z. Ge, L. Rao, S. Gauza, and S. T. Wu, "Modeling of blue phase liquid crystal displays," *J. Display Technol.*, vol. 5, no. 7, pp. 250–256, 2009.

[40] Y. Liu, Y. F. Lan, Q. Hong, and S. T. Wu, "Compensation film designs for high contrast wide-view blue phase liquid crystal displays," *J. Display Technol.*, vol. 10, no. 1, pp. 3–4, 2014.

[41] Z. Ge, M. Jiao, R. Lu, T. X. Wu, S. T. Wu, W. Y. Li, and C. K. Wei, "Wide-view and broadband circular polarizers for transflective liquid crystal displays," *J. Display Technol.*, vol. 4, no. 2, pp. 129–138, 2008.

[42] C. Kim, Y. Park, H. Kong, D. Kim, S. Kang, J. Jang, and S. Kim, "A novel four mask count process architecture for TFT LCDs," in *SID Int. Symp. Dig. Tech. Papers*, 2000, vol. 31, pp. 1006–1009.

[43] S. Choi, J. Cho, K. Y. Han, J. Jang, J. Park, H. Yoon, B. Yoon, S. Ihm, and Y. J. Lim, "Novel four-mask process in the FFS TFT-LCD with optimum multiple-slit design applied by the use of a gray-tone mask," in *SID Int. Symp. Dig. Tech. Papers*, 2005, vol. 36, pp. 284–287.

[44] J. H. Song, D. Kwon, S. Kim, N. Roh, H. Park, Y. Park, D. Kim, C. Jeong, H. Kong, and C. Kim, "Advanced four-mask process architecture for the a-Si TFT array manufacturing method," in *SID Int. Symp. Dig. Tech. Papers*, 2002, vol. 33, pp. 1038–1041.

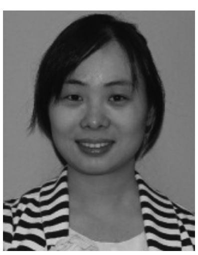

Yan Li received the B.S. and M.S. degrees from Zhejiang University, in 2005 and 2007, respectively, and the Ph.D. degree from the College of Optics and Photonics, University of Central Florida, in 2012.

She has published 30 papers and accumulated more than 350 SCI citations. Her research area includes blue phase liquid crystal devices, 3D displays and fast liquid crystal displays.

Shuaijia Huang received the B.S. degree from Shanghai Jiao Tong University in 2014, where he is currently working toward the M.S. degree.

His research interest includes liquid crystal, adaptive lens and 3D display.

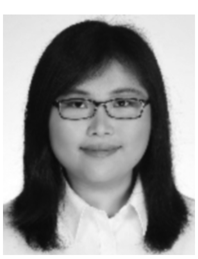

Na Rong received the B.S. degree from Ocean University of China in 2012. She is currently working toward the M.S. degree at Shanghai Jiao Tong University.

Her research interests include holography and 3D display using doped liquid crystal.

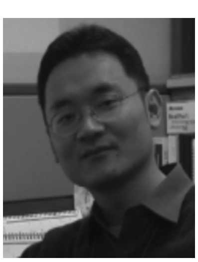

Jian-Gang Lu received the Ph.D. degree from the College of Information Science and Engineering, Zhejiang University, Hangzhou China, in 2003.

He performed research on LC displays with the Next-Generation LCD Research Center, LCD business, Samsung Electronics, from 2003 to 2009. Since 2009, he has been with the National Engineering Laboratory of TFT-LCD Materials and Technologies, Shanghai Jiao Tong University, Shanghai, China, as an Associate Professor. His research includes liquid crystal and polymer material, liquid crystal photonic device, micro-structure optic device, and 3D display.

Chao Ping Chen received the B.S. degree from Shanghai University in 2004 and the M.S. and Ph.D. degrees from Pusan National University, South Korea, in 2006 and 2009, respectively.

He worked at Infovision Optoelectronics and Shanghai Tianma for three odd years before he joined the faculty of Shanghai Jiao Tong University in 2012. His research interests include 3D display, holography, liquid crystal display, and solid state lighting.

Xiao Li received the B.S. and M.S. degrees from the University of Jinan, Jinan, China, in 2006 and 2009, respectively. She is currently working toward the Ph.D. degree at Shanghai Jiao Tong University.

Her research interests include holography and 3D display.

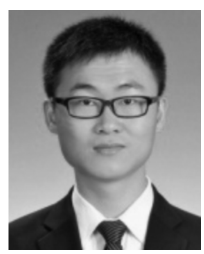

Pengcheng Zhou received the B.S. degree from the University of Science and Technology of China in 2011 and the M.S. degree from the Academy of Opto-Electronics, Chinese Academy of Science, in 2014. He is currently working toward the Ph.D. degree at Shanghai Jiao Tong University.

His research interest includes holography, and 3D display.

Yachao Yuan received the B.S. degree from Wuhan University of Technology in 2012. He is currently working toward the M.S. degree at Shanghai Jiao Tong University.

His research interest includes liquid crystal, holographic data storage and 3D display.

Shuxin Liu received the B.S. degree from University of Electronic Science and Technology of China in 2014. He is currently working toward the Ph.D. degree at Shanghai Jiao Tong University.

His research interests include holography and 3D display.

Gufeng He received the B.S. degree in polymer science and engineering from the University of Science and Technology of China (USTC) and the M.S. and Ph.D. degrees in organic optoelectronic devices from the Institute of Chemistry, Chinese Academy of Sciences.

From 2002 to 2005, he performed post-doctoral research on high-performance organic light-emitting devices at the University of Technology at Dresden (TU-Dresden), Germany. Thereafter, he worked at Novaled AG as a Senior Scientist for five years on high-efficiency and long-lifetime white OLED development for display and lighting applications. In 2010, he became a Professor with Shanghai Jiao Tong University in China. His main research interests are organic optoelectronic functional materials and devices.

Yikai Su (SM'07) received the B.S. degree from the Hefei University of Technology, China in 1991, the M.S. degree from the Beijing University of Aeronautics and Astronautics, China in 1994, and the Ph.D. degree in electrical engineering from Northwestern University, Evanston, IL, USA, in 2001.

Prior to joining Shanghai Jiao Tong University (SJTU) in 2004, he worked at Bell Laboratories, NJ, USA. He is currently a Full Professor with the Department of Electronic Engineering. He has published more than 200 papers. He serves as the Director of the Center for Opto-electronic Materials and Devices and Vice Director of the National Engineering Lab for TFT-LCD materials and technologies.

Prof. Su is a member of OSA and SID. He has given invited talks at Photonics West, SPIE Opto+Photonics, IDMC, CLEO-PR, OLC, ADMD, DH etc. He serves as the chapter chair of IEEE Photonics Society in Shanghai, and a faculty advisor of the SJTU OSA student chapter. His research area covers micro and nano photonic devices and real-time holographic 3D display. He serves as an advisory editorial board member of *Advanced Optical Materials* and an associate editor of *Photonics Research*. He was a Topical Editor of *Optics Letters*, a Feature editor of *Applied Optics*, and a Guest Editor of the IEEE JOURNAL OF SELECTED TOPICS IN QUANTUM ELECTRONICS 2008.